

# Gas-liquid phase coexistence and crossover behavior of binary ionic fluids with screened Coulomb interactions

O. Patsahan

*Institute for Condensed Matter Physics of the National Academy of Sciences of Ukraine,  
1 Svientsitskii St., 79011 Lviv, Ukraine*

(Dated: July 17, 2014)

## Abstract

We study the effects of an interaction range on the gas-liquid phase diagram and the crossover behavior of a simple model of ionic fluids: an equimolar binary mixture of equisized hard spheres interacting through screened Coulomb potentials which are repulsive between particles of the same species and attractive between particles of different species. Using the collective variables theory, we find explicit expressions for the relevant coefficients of the effective  $\varphi^4$  Ginzburg-Landau Hamiltonian in a one-loop approximation. Within the framework of this approximation, we calculate the critical parameters and gas-liquid phase diagrams for varying inverse screening length  $z$ . Both the critical temperature scaled by the Yukawa potential contact value and the critical density rapidly decrease with an increase of the interaction range (a decrease of  $z$ ) and then for  $z < 0.05$  they slowly approach the values found for a restricted primitive model (RPM). We find that gas-liquid coexistence region reduces with an increase of  $z$  and completely vanishes at  $z \simeq 2.78$ . Our results clearly show that an increase in the interaction range leads to a decrease of the crossover temperature. For  $z \simeq 0.01$ , the crossover temperature is the same as for the RPM.

## I. INTRODUCTION

The nature of phase separation and criticality in ionic fluids with the dominant Coulomb interactions (e.g., molten salts and electrolytes in solvents of low dielectric constant) has been an outstanding experimental and theoretical issue for many years. Electrostatic correlations are also known to play an important role in many other technologically relevant systems such as charge-colloidal suspensions, room-temperature ionic liquids and micellar solutions of ionic surfactants. Now, a generally accepted idea is that the gas-liquid and liquid-liquid critical points in ionic fluids belong to the universal class of a three-dimensional Ising model [1–3]. Nevertheless, the crossover from the mean-field-like behavior to the Ising model criticality when approaching the critical point remains a challenging problem for theory, simulations and experiments [2, 3].

The most commonly studied theoretical model of ionic fluids is a restricted primitive model (RPM), which consists of equal numbers of equisized positively and negatively charged hard spheres immersed in a structureless dielectric continuum. The RPM undergoes a gas-liquid-like phase transition at low temperature and low density [4–7]. Theoretical [8–10] and numerical [11–14] investigations of the gas-liquid criticality in the RPM have provided strong evidence for an Ising universal class. However, an issue of the width of the critical region was not addressed in these works. On the other hand, the Ginzburg criterion [15–17] was used in Ref. [18–22] in order to study the crossover from the mean-field to asymptotic regime, but the obtained results failed to give a clear answer to the question of the extent of the crossover region in the model.

Recently, using the method of collective variables (CVs) [23–26], we have derived the Landau-Ginzburg (LG) Hamiltonian for the model of ionic fluids which includes, besides Coulomb interactions, short-range attractive interactions [27]. An important feature of the developed approach is that it enables us to obtain all the relevant coefficients, including the square-gradient term, within the framework of the same approximation. The Ginzburg temperature for the RPM, calculated using this theory turned out to be about 20 times smaller than for a one-component nonionic model. Furthermore, the results obtained for the RPM supplemented by short-range attractive interactions have shown that the Ginzburg temperature approaches the value found for the RPM when the strength of Coulomb interactions becomes sufficiently large. These results suggest the key role of Coulomb interactions in

the reduction of the crossover region. Nevertheless, the study of the effect of an interaction range on the Ginzburg temperature is needed in order to gain a better understanding of the crossover behavior in ionic fluids.

In the present work, we extend the theory to the binary ionic model with screened Coulomb interactions. Specifically, we consider a two-component system of particles labeled 1 and 2, such that the interaction potential between a particle of species  $\alpha$  and one of the species  $\beta$  at a distance  $r$  apart is as follows:

$$u_{\alpha\beta}(r) = \begin{cases} \infty, & r < \sigma \\ (-1)^{\alpha+\beta} K \frac{\exp(-z(r/\sigma - 1))}{r/\sigma}, & r \geq \sigma \end{cases}, \quad (1)$$

where  $\alpha, \beta = (1, 2)$ . For  $K > 0$ , Eq. (1) describes a symmetrical mixture of hard spheres of the same diameter  $\sigma$  in which the like particles interact through a repulsive Yukawa potential for  $r > \sigma$ , and the unlike particles interact through the opposite attractive Yukawa potential for  $r > \sigma$ . We restrict our consideration to the case where the number densities of species 1 and 2 are the same, i.e.,  $\rho_1 = \rho_2 = \rho/2$ . For  $K = (q)^2/\epsilon$ , the model (1) is called a Yukawa restricted primitive model (YRPM). In this case,  $q_+ = -q_- = q$  is the charge magnitude and  $\epsilon$  is the dielectric constant of the medium. In the limit  $z \rightarrow \infty$ , the YRPM reduces to a hard sphere model whereas the RPM is recovered by taking the limit  $z \rightarrow 0$ . Thus, the YRPM can provide a basis for the study of the nature of phase and critical behavior in ionic fluids and in partially ionic fluids.

It is worth noting that the YRPM is often used to model a system of oppositely charged colloids [28–31]. The effective (screened) colloid-colloid interactions in such a system are due to the presence of coions and counterions in the solvent. In this case,  $K$  and  $z$  take the form:  $K/k_B T = Z^2 \lambda_B / (1 + \kappa_D \sigma / 2)^2 / \sigma$  and  $z = \kappa_D \sigma$ , where  $\kappa_D = \sqrt{8\pi \lambda_B \rho_s}$  is the inverse Debye screening length,  $\lambda_B = e^2 / \epsilon_s k_B T$  is the Bjerrum length,  $\rho_s$  is the salt concentration and  $\epsilon_s$  is the dielectric constant of the solvent. In a colloid system, the range of interaction can be modified by changing the salt concentration.

Whereas the effect of an interaction range on the gas-liquid phase separation of a simple one-component fluid has been extensively studied (see Ref. [32] and references herein), as far as we know there are only a few works addressing this issue for the case of the YRPM [10, 30, 33, 34]. In particular, the evolution of the gas-liquid phase diagram of the YRPM as a function of the interaction range was theoretically studied using the integral equation

methods [33, 34] and the hierarchical reference theory (HRT) [10]. The results obtained from the generalized mean-spherical approximation (GMSA) show that both the critical density and the critical temperature increase above the corresponding values for the RPM when  $z$  increases [33]. Moreover, the GMSA predicts a nonmonotonous behavior of the critical temperature as a function of  $z$ : the critical temperature attains a maximum at  $z \approx 4$ . In Ref. [33], the attention was focused on several values of  $z$ ,  $z = 0, 1.5075, 3, 4, 5$  and  $6$ , and the gas-liquid coexistence was found for all the listed values. The highest value for which the gas-liquid coexistence was found within the framework of integral equation methods is  $z = 25$  with the MSA [34]. In Ref. [10] the main emphasis is made on the critical behavior of the model.

Simulations predict a rich phase diagram involving a gas-liquid phase separation as well as several crystalline phases, which is in agreement with experimental confocal microscopy data for charge-stabilized colloidal suspensions [28–31]. These studies indicate a sensitivity of the phase diagram of the YRPM to the variation of  $z$ . Unlike theoretical predictions [33, 34], it is found [30] that the gas-liquid separation is not stable with respect to gas-solid coexistence for  $z > 4$ .

The purpose of the present paper is to study the effects of the interaction range on the gas-liquid phase diagram and the Ginzburg temperature of the YRPM. To this end, following Ref. [27], we find analytical expressions for all the relevant coefficients of the LG Hamiltonian in a one-loop approximation. Based on these expressions, first we calculate the gas-liquid critical parameters, spinodals and coexistence curves of the model for  $0.001 \leq z \leq 2.781$ . Remarkably, there is no gas-liquid critical point for  $z \geq 2.782$  in the approximation considered. Our discussion also involves an analysis of the dependence of the coefficients of the effective Hamiltonian on the interaction range. Applying the Ginzburg criterion, we find that the reduced Ginzburg temperature decreases with an increase of the interaction range approaching the RPM value for  $z \simeq 0.01$ . The present analysis also indicates the presence of a tricritical point at  $z = 2.781$ .

The paper is organized as follows. A brief description of the formalism is given in Sec. 2. The results for the gas-liquid phase diagram and the critical parameters are presented in Sec. 3. In Sec 4 we discuss the effect of the interaction range on the crossover behavior of the YRPM. Concluding remarks are made in Sec. 5.

## II. THEORY

### A. Functional representation of the grand partition function

We start with the YRPM and present the interaction potential (1) in the form:

$$u_{\alpha\beta}(r) = \phi^{\text{HS}}(r) + \phi_{\alpha\beta}^Y(r), \quad (2)$$

where  $\phi^{\text{HS}}(r)$  is the interaction potential between the two hard spheres of diameter  $\sigma$ . Thermodynamic and structural properties of the system interacting through the potential  $\phi^{\text{HS}}(r)$  are assumed to be known. Therefore, the one-component hard-sphere model is regarded as the reference system.  $\phi_{\alpha\beta}^Y(r)$  are the screened Coulomb potentials. Figure 1 shows the shape of the interaction potentials  $\phi_{\alpha\beta}^Y(r)/K$  for different values of the inverse screening length.

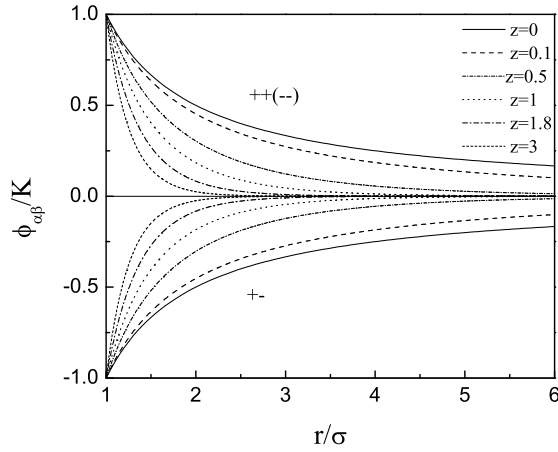


FIG. 1. Interaction potentials  $\phi_{\alpha\beta}^Y(r)/K$  for different values of the inverse screening length  $z$ .

The model under consideration is at equilibrium in the grand canonical ensemble,  $\beta = (k_B T)^{-1}$  is the inverse temperature, and  $\nu_\alpha = \beta \mu_\alpha$  ( $\nu_\alpha = \nu_\beta = \nu$ ) is the dimensionless chemical potential of the  $\alpha$ th species. Using the CV method we present the grand partition function of the model in the form of a functional integral [26, 27]:

$$\begin{aligned} \Xi = \Xi_{\text{HS}} \exp [\Delta \nu_N \langle N \rangle_{\text{HS}}] \int (d\rho)(d\omega) \exp \left[ \Delta \nu_N \rho_{0,N} - \frac{\beta}{2V} \sum_{\mathbf{k}} \tilde{\phi}^Y(k) \rho_{\mathbf{k},Q} \rho_{-\mathbf{k},Q} \right. \\ \left. + i \sum_{\mathbf{k}} (\omega_{\mathbf{k},N} \rho_{\mathbf{k},N} + \omega_{\mathbf{k},Q} \rho_{\mathbf{k},Q}) + \sum_{n \geq 2} \frac{(-i)^n}{n!} \sum_{i_n \geq 0} \sum_{\mathbf{k}_1, \dots, \mathbf{k}_n} \mathfrak{M}_n^{(i_n)}(k_1, \dots, k_n) \right. \\ \left. \times \omega_{\mathbf{k}_1,Q} \dots \omega_{\mathbf{k}_{i_n},Q} \omega_{\mathbf{k}_{i_n+1},N} \dots \omega_{\mathbf{k}_n,N} \delta_{\mathbf{k}_1 + \dots + \mathbf{k}_n} \right]. \end{aligned} \quad (3)$$

Here,  $\rho_{\mathbf{k},N}$  and  $\rho_{\mathbf{k},Q}$  are the CVs which describe fluctuations of the total number density and the charge density (or relative number density), respectively:

$$\rho_{\mathbf{k},N} = \rho_{\mathbf{k},+} + \rho_{\mathbf{k},-}, \quad \rho_{\mathbf{k},Q} = \rho_{\mathbf{k},+} - \rho_{\mathbf{k},-}.$$

CV  $\rho_{\mathbf{k},\alpha} = \rho_{\mathbf{k},\alpha}^c - i\rho_{\mathbf{k},\alpha}^s$  describes the value of the  $\mathbf{k}$ -th fluctuation mode of the number density of the  $\alpha$ th species, the indices  $c$  and  $s$  denote real and imaginary parts of  $\rho_{\mathbf{k},\alpha}$ ; CVs  $\omega_N$  and  $\omega_Q$  are conjugate to  $\rho_N$  and  $\rho_Q$ , respectively.  $(d\rho)$  and  $(d\omega)$  denote volume elements of the CV phase space:

$$(d\rho) = \prod_{A=N,Q} d\rho_{0,A} \prod'_{\mathbf{k} \neq 0} d\rho_{\mathbf{k},A}^c d\rho_{\mathbf{k},A}^s, \quad (d\omega) = \prod_{A=N,Q} d\omega_{0,A} \prod'_{\mathbf{k} \neq 0} d\omega_{\mathbf{k},A}^c d\omega_{\mathbf{k},A}^s$$

and the product over  $\mathbf{k}$  is performed in the upper semi-space ( $\rho_{-\mathbf{k},A} = \rho_{\mathbf{k},A}^*$ ,  $\omega_{-\mathbf{k},A} = \omega_{\mathbf{k},A}^*$ ).

$\tilde{\phi}^Y(k)$  is the Fourier transform of the repulsive potential  $\phi_{\alpha\alpha}^Y(r) = \phi^Y(r)$ , where  $\phi^Y(r) = K\sigma \exp[-z(r/\sigma - 1)]/r$ . Here we use the Weeks-Chandler-Andersen regularization of the potential  $\phi^Y(r)$  inside the hard core [35]. In this case,  $\tilde{\phi}^Y(k)$  has the form

$$\tilde{\phi}^Y(x) = \frac{4\pi K\sigma^3}{x^3(z^2 + x^2)} \bar{f}(x), \quad (4)$$

where

$$\bar{f}(x) = [z^2 + x^2(1 + z)] \sin(x) - xz^2 \cos(x), \quad (5)$$

and  $x = k\sigma$ . Due to symmetry in the YRPM, the Hamiltonian in (3) does not include direct pair interactions of number density fluctuations.

$\Xi_{\text{HS}}$  is the grand partition function of the one-component hard-sphere model with the dimensional chemical potential  $\nu_{\text{HS}}$ .  $\Delta\nu_N = \bar{\nu} - \nu_{\text{HS}}$  where

$$\bar{\nu} = \bar{\nu}_\alpha = \nu_\alpha + \frac{\beta}{2V} \sum_{\mathbf{k}} \tilde{\phi}^Y(k), \quad \alpha = (1, 2). \quad (6)$$

Hereafter, the subscript HS refers to the hard-sphere system.

The cumulants  $\mathfrak{M}_n^{(i_n)}$  are expressed in terms of the Fourier transforms of the connected correlation functions of the hard-sphere system [26].  $\delta_{\mathbf{k}_1 + \dots + \mathbf{k}_n}$  is the Kronecker symbol. In the case of the YRPM, we have the following recurrence relations for the cumulants  $\mathfrak{M}_n^{(i_n)}$  [26]:

$$\begin{aligned} \mathfrak{M}_n^{(0)} &= \tilde{G}_{n,\text{HS}}, & \mathfrak{M}_n^{(1)} &= 0, \\ \mathfrak{M}_n^{(2)} &= \tilde{G}_{n-1,\text{HS}}, & \mathfrak{M}_n^{(3)} &= 0, \\ \mathfrak{M}_n^{(4)} &= 3\tilde{G}_{n-2,\text{HS}} - 2\tilde{G}_{n-1,\text{HS}}, \end{aligned}$$

where  $\tilde{G}_{n,\text{HS}}$  denotes the Fourier transform of the  $n$ -particle connected correlation function of a one-component hard-sphere system. In general, the dependence of  $\tilde{G}_{n,\text{HS}}$  on the wave numbers  $k_i$  is very complicated. Hereafter we use the following approximation for  $\tilde{G}_{n,\text{HS}}$

$$\begin{aligned}\tilde{G}_{2,\text{HS}}(k) &\simeq \tilde{G}_{2,\text{HS}}(0) + \frac{k^2}{2} \tilde{G}_{2,\text{HS}}^{(2)}, \\ \tilde{G}_{n,\text{HS}}(k_1, \dots, k_n) &\simeq \tilde{G}_{n,\text{HS}}(0, \dots) \quad \text{for } n \geq 3,\end{aligned}$$

where the superscript (2) denotes the second-order derivative with respect to the wave vector.

## B. Gaussian approximation

Now we consider the Gaussian approximation of  $\Xi$  setting in Eq. (3)  $\mathfrak{M}_n^{(i_n)} \equiv 0$  for  $n \geq 3$ . Then, after integration over  $\omega_{\mathbf{k},N}$  and  $\omega_{\mathbf{k},Q}$  we obtain

$$\Xi_{\text{G}} = \Xi' \int (d\rho) \exp \left\{ \Delta \nu_N \rho_{0,N} - \frac{1}{2} \sum_{\mathbf{k}} \left[ a_2^{(0)}(k) \rho_{\mathbf{k},N} \rho_{-\mathbf{k},N} + a_2^{(2)}(k) \rho_{\mathbf{k},Q} \rho_{-\mathbf{k},Q} \right] \right\},$$

where

$$\Xi' = \Xi_{\text{HS}} \exp [\Delta \nu_N \langle N \rangle_{\text{HS}}] \prod_{\mathbf{k}} \left[ \mathfrak{M}_2^{(0)} \mathfrak{M}_2^{(2)} \right]^{-1/2},$$

and

$$a_2^{(0)}(k) = \left[ \mathfrak{M}_2^{(0)}(k) \right]^{-1}, \quad a_2^{(2)}(k) = \frac{\beta}{V} \tilde{\phi}^Y(k) + \left[ \mathfrak{M}_1^{(0)} \right]^{-1}. \quad (7)$$

It follows from Eq. (7) that  $a_2^{(0)}(k)$  never vanishes for physical values of the density. The fact that the YRPM like the RPM does not undergo the gas-liquid instability in the Gaussian approximation is due to the absence of direct pair interactions of density fluctuations as well as to the neglect of the effect of non-direct correlations via a charge subsystem at this level of consideration. By contrast,  $a_2^{(2)}(k)$  can be equal to zero at  $k = k^* \neq 0$ , where  $k^*$  is determined from the condition  $\partial a_2^{(2)} / \partial k = 0$ . The locus in the phase diagram at which  $a_2^{(2)}(k = k^*) = 0$  is called the  $\lambda$ -line [36, 37] in order to distinguish it from the spinodal line for which  $k^* = 0$ . On the  $\lambda$ -line the fluid becomes unstable with respect to the charge ordering indicating that there can be a phase transition to an ordered phase. For the RPM ( $z = 0$ ), it was found that in the presence of fluctuations the  $\lambda$ -line disappears and, instead, a first-order phase transition to an ionic crystal appears [38].

### C. Effective Ginzburg-Landau Hamiltonian

We consider the model (2) near the gas-liquid critical point. In this case, the phase space of CVs  $\rho_{\mathbf{k},N}$  contains CV  $\rho_{0,N}$  related to the order parameter. In order to obtain the effective Hamiltonian in terms of  $\rho_{\mathbf{k},N}$ , one should integrate in Eq. (3) over CVs  $\omega_{\mathbf{k},N}$ ,  $\omega_{\mathbf{k},Q}$ , and  $\rho_{\mathbf{k},Q}$ . A detailed derivation of this type of Hamiltonian is given in Ref. [27]. Using the results of Ref. [27], we can write an expression for the effective  $\varphi^4$  LG Hamiltonian of the model under consideration

$$\begin{aligned} \mathcal{H}^{eff} = & a_{1,0}\rho_{0,N} + \frac{1}{2!\langle N \rangle} \sum_{\mathbf{k}} (a_{2,0} + k^2 a_{2,2}) \rho_{\mathbf{k},N} \rho_{-\mathbf{k},N} + \frac{1}{3!\langle N \rangle^2} \sum_{\mathbf{k}_1, \mathbf{k}_2} a_{3,0} \\ & \times \rho_{\mathbf{k}_1,N} \rho_{\mathbf{k}_2,N} \rho_{-\mathbf{k}_1-\mathbf{k}_2,N} + \frac{1}{4!\langle N \rangle^3} \sum_{\mathbf{k}_1, \mathbf{k}_2, \mathbf{k}_3} a_{4,0} \rho_{\mathbf{k}_1,N} \rho_{\mathbf{k}_2,N} \rho_{\mathbf{k}_3,N} \rho_{-\mathbf{k}_1-\mathbf{k}_2-\mathbf{k}_3,N} \end{aligned} \quad (8)$$

with the coefficients having the following form in a one-loop approximation:

$$a_{1,0} = -\Delta\nu_N - \tilde{\mathcal{C}}_{1,Y} \quad (9)$$

$$a_{n,0} = -\rho^{n-1} \tilde{\mathcal{C}}_{n,\text{HS}} - \rho^{n-1} \tilde{\mathcal{C}}_{n,Y} \quad (10)$$

$$a_{2,2} = -\frac{1}{2}\rho \tilde{\mathcal{C}}_{2,\text{HS}}^{(2)} - \frac{1}{4\langle N \rangle} \sum_{\mathbf{q}} \tilde{g}_Y^{(2)}(\mathbf{q}) [1 + \tilde{g}_Y(\mathbf{q})]. \quad (11)$$

Here, we introduce the following notations. The superscript (2) in Eq. (11) denotes the second-order derivative with respect to the wave vector.  $\tilde{\mathcal{C}}_{n,\text{HS}}$  is the Fourier transform of the  $n$ -particle direct correlation function of a one-component hard-sphere system at  $k=0$ , and  $\rho = \langle N \rangle/V$  is the number density. Explicit expressions for  $\tilde{\mathcal{C}}_{n,\text{HS}}$  and  $\tilde{\mathcal{C}}_{2,\text{HS}}^{(2)}$  for  $n \leq 4$  in the Percus Yevick (PY) approximation are given in Ref. [27] (see Appendix in Ref. [27]).

The second term on the right-hand side of Eqs. (9)–(11) arises from the integration over CVs  $\rho_{\mathbf{k},Q}$  and  $\omega_{\mathbf{k},Q}$ . In particular,  $\rho^{n-1}\tilde{\mathcal{C}}_{n,Y}$  reads

$$\rho^{n-1}\tilde{\mathcal{C}}_{n,Y} = \frac{(n-1)!}{2} \frac{1}{\langle N \rangle} \sum_{\mathbf{q}} [\tilde{g}_Y(\mathbf{q})]^n, \quad (12)$$

where

$$\tilde{g}_Y(\mathbf{q}) = -\frac{\beta\rho\tilde{\phi}^Y(\mathbf{q})}{1 + \beta\rho\tilde{\phi}^Y(\mathbf{q})} \quad (13)$$

with  $\tilde{\phi}^Y(\mathbf{q})$  given by Eq. (4).



Taking into account Eqs. (4) and (13), one can obtain the following explicit expressions for  $\rho^{n-1}\tilde{\mathcal{C}}_{n,Y}$ :

$$-\rho^{n-1}\tilde{\mathcal{C}}_{n,Y} = \frac{(n-1)!(-24\eta)^{n-1}}{\pi} \int_0^\infty x^2 \left[ \frac{\bar{f}(x)}{T^*x^3(z^2 + x^2) + 24\eta\bar{f}(x)} \right]^n dx, \quad (14)$$

where  $\bar{f}(x)$  is given by Eq. (5). Hereafter, the following reduced units are introduced for the temperature

$$T^* = (\beta K)^{-1} \quad (15)$$

and for the density

$$\eta = \frac{\pi}{6}\rho^*, \quad \rho^* = \rho\sigma^3. \quad (16)$$

The explicit expression for the second term in Eq. (11) is too long to be presented herein. We only emphasize that although the Hamiltonian in Eq. (3) does not include direct pair interactions of number density fluctuations, the effective short-range attraction does appear in the effective Hamiltonian (8). Moreover, in the limit of charged point particles, i.e.,  $z = 0$  and  $\sigma = 0$ , the expression for  $a_{2,2}$  leads to the correct result for the density-density correlation length (see Refs. [27, 39]).

The term  $\Delta\nu_N$  in Eq. (9) can be rewritten as follows [see Eq. (6)]:

$$\Delta\nu_N = \nu - \nu_{\text{HS}} + \frac{1}{2T^*}. \quad (17)$$

Summarizing, the expressions for coefficients  $a_{2,0}$ ,  $a_{3,0}$ ,  $a_{4,0}$ , and  $a_{2,2}$  consist of two terms. While the first term depends solely on the characteristics of a hard-sphere system, the second term is of a mixed type and takes into account the charge-charge (concentration-concentration) correlations. Coefficient  $a_{1,0}$  is the excess part of the chemical potential  $\nu$ , and the equation  $a_{1,0} = 0$  yields the chemical potential in a one-loop approximation. It follows from Eqs. (9), (14) and (17) that

$$\nu = \nu_{\text{HS}} - \frac{1}{2T^*} + \frac{1}{\pi} \int_0^\infty \frac{x^2 \bar{f}(x)}{T^*x^3(z^2 + x^2) + 24\eta\bar{f}(x)} dx. \quad (18)$$

where  $\nu_{\text{HS}}$  includes ideal and hard-sphere parts. Using the above equation, one can obtain the gas-liquid diagram in the mean-field approximation.

### III. GAS-LIQUID PHASE TRANSITION

In this section we study the gas-liquid phase diagram of the model (2) using Eq. (10) and Eqs. (14)-(18). First, we consider the critical point. At the critical point, the system of

equations

$$a_{2,0}(\rho_c, T_c) = 0, \quad a_{3,0}(\rho_c, T_c) = 0 \quad (19)$$

holds yielding the critical temperature and the critical density for the fixed value of  $z$ . Using Eqs. (5) and (14), these equations can be rewritten as follows:

$$\frac{(1+2\eta)^2}{(1-\eta)^4} - \frac{24\eta}{\pi} \int_0^\infty \frac{x^2 \bar{f}^2(x) dx}{[T^* x^3 (z^2 + x^2) + 24\eta \bar{f}(x)]^2} = 0, \quad (20)$$

$$\frac{(1-7\eta-6\eta^2)(1+2\eta)}{(1-\eta)^5} - \frac{1152\eta^2}{\pi} \int_0^\infty \frac{x^2 \bar{f}^3(x) dx}{[T^* x^3 (z^2 + x^2) + 24\eta \bar{f}(x)]^3} = 0. \quad (21)$$

Here, the PY approximation is used for  $\tilde{\mathcal{C}}_{n,\text{HS}}$ . It is worth noting that Eq. (20) yields the spinodal curve.

Solving Eqs. (20) and (21) we obtain the critical temperature  $T_c^*$  and the critical density  $\rho_c^*$  for  $z$  ranging from  $z = 0.001$  to  $z = 2.781$ . At  $z \geq 2.782$ , the system of equations (20) and (21) has no solution in the region of the gas-liquid phase transition indicating a disappearance of the critical point. The dependence of  $T_c^*$  and  $\rho_c^*$  on the parameter  $z^{-1}$  measuring the interaction range is displayed in Figs. 2 and 3, respectively. As is seen, the reduced critical temperature  $T_c^*$  rapidly decreases with an increase of the interaction range for  $z^{-1} \leq 20$  and then slowly approaches the critical temperature of the RPM ( $T_c^* = 0.08446$ ). The reduced critical density  $\rho_c^*$  demonstrates a sharp decrease in the region  $z^{-1} \leq 10$  reaching the RPM critical value for  $z^{-1} \simeq 100$ . A decrease of both the critical temperature and the critical density expressed in the same reduced units is observed in Ref. [30].

We calculate the spinodal curves for different values of  $z$  using Eq. (20). The results are presented in the  $(T^*, \eta)$  plane in Fig. 4. As is seen, the spinodals change their shape with the variation of the interaction range. For small values of  $z$ , the curves have a noticeable maximum at small  $\eta$  and change their run passing through a minimum. The maximum point of the spinodal coincides with the gas-liquid critical point. The second positive slope of spinodal curves appearing at higher densities indicates another type of phase instability induced by the charge ordering. We suggest that this branch of the spinodal should be an indication of the pretransitional effects associated with crystallization. For the system of oppositely charged colloids, a broad fluid–CsCl crystal phase coexistence is found experimentally [29] and by computer simulations [29, 30]. Moreover, it is shown that fluid-solid phase diagrams of the YRPM and the RPM are qualitatively similar [29]. When  $z$  increases, the maximum of spinodals moves to higher densities, becomes flatter and finally disappears

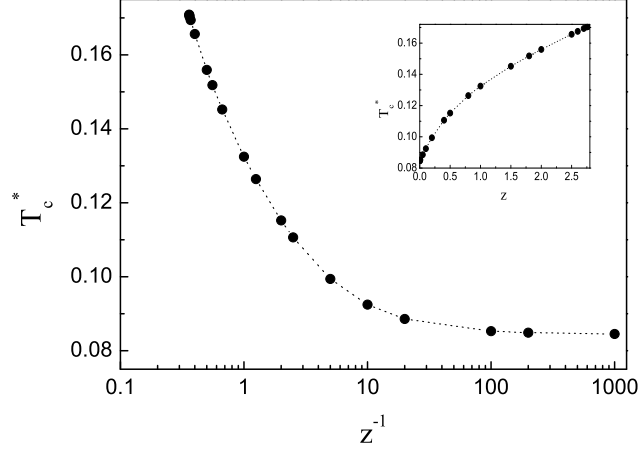


FIG. 2. Reduced critical temperature  $T_c^*$  [Eq. (15)] of the YRPM as a function of the interaction range. The inset shows  $T_c^*$  as a function of  $z$ . The line is a guide to the eye.

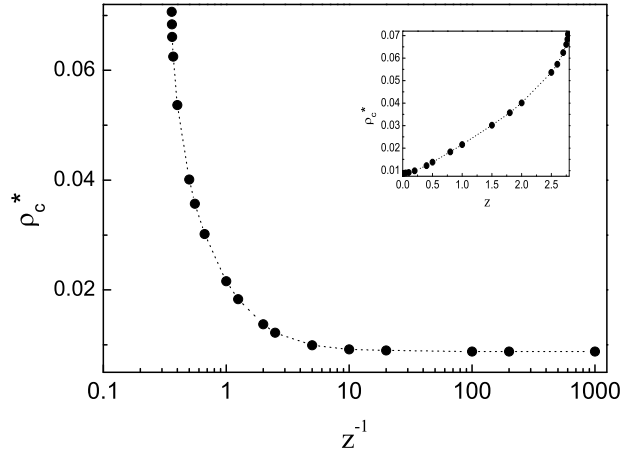


FIG. 3. Reduced critical density [Eq. (16)] of the YRPM as a function of the interaction range. The inset shows  $\rho_c^*$  as a function of  $z$ . The line is a guide to the eye.

at  $z > 2.781$ . At  $z = 2.781$ , the gas-liquid critical point merges with the spinodal branch induced by the charge ordering.

To calculate the coexistence curves, we use Eq. (18) for the chemical potential and employ the Maxwell double-tangent construction. Figure 5 shows both the coexistence curves (solid lines) and spinodals (dashed lines) in the  $(T^*, \eta)$  plane for a set of  $z$  values. As is seen, the region of gas-liquid coexistence reduces with an increase of  $z$ . Furthermore, the coexistence curves become very flat for  $z \geq 2.7$ . This means that the liquid phase becomes more and more difficult to observe in this domain of  $z$ . For  $z > 2.781$ , no critical point can be

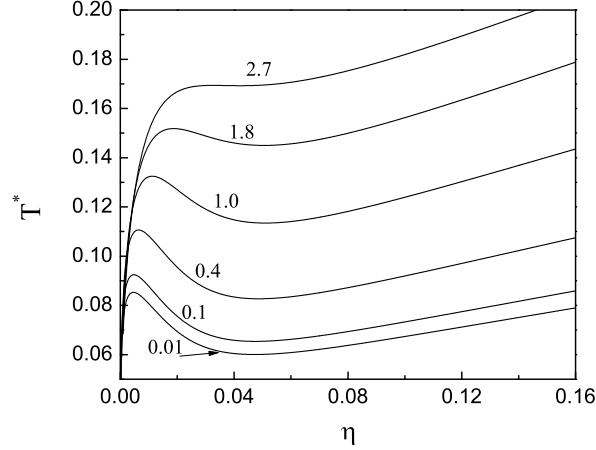


FIG. 4. Spinodal curves of the YRPM for  $z$  ranging from 0.01 to 2.7 in the  $(T^*, \eta)$  representation.

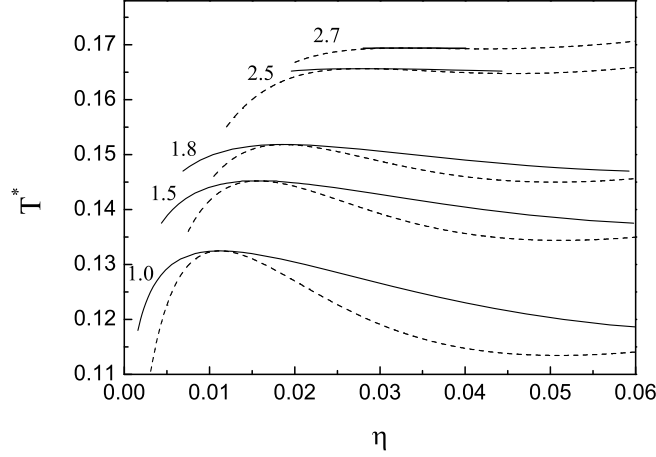


FIG. 5. Coexistence curves (solid) and spinodal curves (dashed) of the YRPM for  $z$  ranging from 1.0 to 2.7 in the  $(T^*, \eta)$  representation.

calculated and  $z = 2.781$  can be considered as the limit value for gas-liquid phase separation in the approximation considered in this paper. We recall that the limit value for a stable gas-liquid separation obtained in simulations is  $z = 4$  [30].

#### IV. THE CROSSOVER TEMPERATURE

In this section, we study the effect of the interaction range on the temperature region in which the crossover from classical behavior to Ising-like critical behavior occurs. To this end, we use the Ginzburg criterion [15, 16]. This criterion defines the reduced Ginzburg temperature  $t_G$  which marks a lower bound of the temperature region where a mean-field

description is self-consistent. For  $|t| \ll t_G$  where  $|t| = |T - T_c|/T_c$ , Ising critical behavior should be exhibited. Therefore, it is reasonable to take the reduced Ginzburg temperature as an estimate of the crossover temperature [1, 17, 19].

The Ginzburg temperature expressed in terms of coefficients of the Hamiltonian (8) reads [19]

$$t_G = \frac{1}{32\pi^2} \frac{a_{4,0}^2}{a_{2,t} a_{2,2}^3}, \quad (22)$$

where  $a_{2,t} = \partial a_{2,0}/\partial t|_{t=0}$ . Taking into account Eqs. (10) and (14), one can obtain for  $a_{2,t}$

$$a_{2,t} = \frac{48\eta T_c^*}{\pi} \int_0^\infty \frac{x^5(z^2 + x^2)\bar{f}^2(x)}{(T_c^* x^3(z^2 + x^2) + 24\eta\bar{f}(x))^3} dx, \quad (23)$$

where  $\bar{f}$  is given by (5).

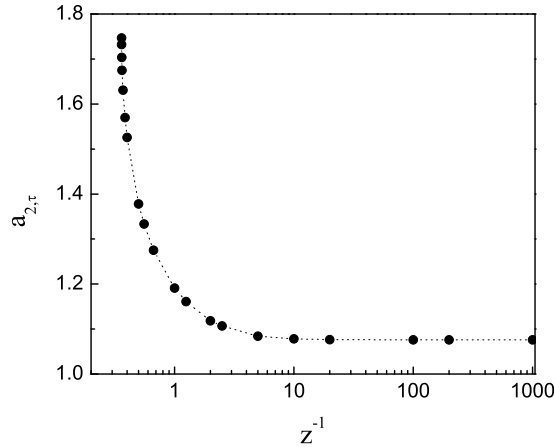


FIG. 6. The coefficient  $a_{2,t}$  as a function of the interaction range  $z^{-1}$ . The line is a guide to the eye.

The relevant coefficients of the LG Hamiltonian are calculated at  $T^* = T_c^*$  and  $\rho^* = \rho_c^*$  using Eqs. (10), (11), (14), and (23). It is instructive to view the coefficients  $a_{2,t}$ ,  $a_{2,2}$ , and  $a_{4,0}$  as functions of  $z^{-1}$ . Figures 6–8 show the dependence of coefficients on the interaction range. While  $a_{2,t}$  is a decreasing function of  $z^{-1}$ , the other two coefficients demonstrate a nonmonotonous behavior. It is worth noting that  $a_{2,t} > 1$  for the whole range of  $z$  for which coexistence exists. The coefficient  $a_{2,2}$  corresponds to a squared range of the effective density-density attraction. Being nearly constant for  $z \leq 0.1$ ,  $a_{2,2}$  decreases for larger values of  $z$  and attains a minimum at  $z \simeq 1.8$ . Then, it slightly increases in the range  $1.8 < z < 2.78$ . The coefficient  $a_{4,0}$  has a maximum at  $z \simeq 1.5$  and then (for  $z > 1.5$ ) sharply tends to

zero indicating the presence of a tricritical point at  $z = 2.781$  for which our estimate is  $T_c^* = 0.1709$ ,  $\rho_c^* = 0.0718$ . For  $z \lesssim 0.01$  ( $z^{-1} \gtrsim 100$ ), all three coefficients become equal to the corresponding coefficients of the RPM [27].

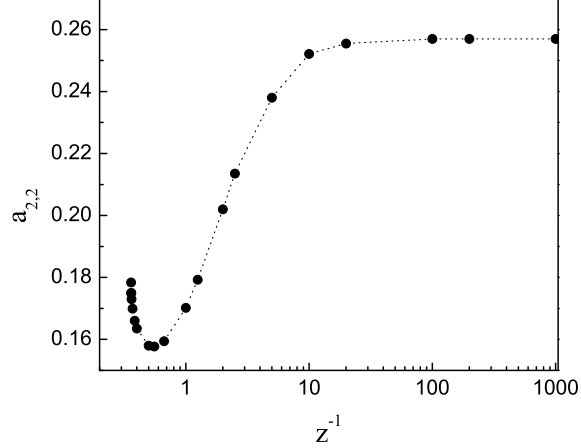


FIG. 7. Coefficient  $a_{2,2}$  as a function of the interaction range  $z^{-1}$ . The line is a guide to the eye.

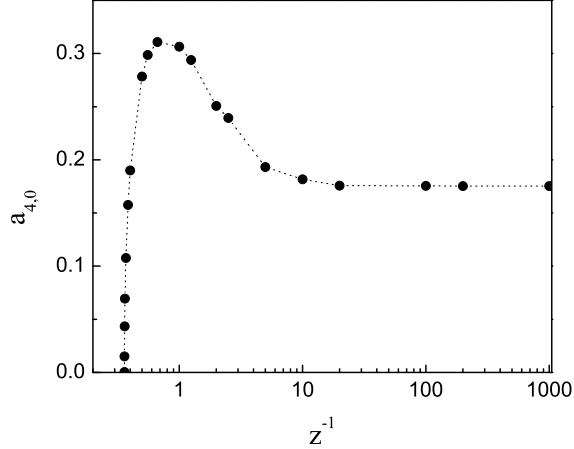


FIG. 8. Coefficient  $a_{4,0}$  as a function of the interaction range  $z^{-1}$ . The line is a guide to the eye.

The dependence of the reduced Ginzburg temperature  $t_G$  on the interaction range is shown in Fig. 9. For  $z \simeq 0.01$  ( $z^{-1} \simeq 100$ ), the reduced Ginzburg temperature approaches the value  $t_G = 0.0053$  obtained for the RPM [27]. For large values of  $z$  (small  $z^{-1}$ ),  $t_G$  shows a nonmonotonous behavior passing through a sharp maximum at  $z \simeq 1.5$  and approaching zero at  $z \simeq 2.78$ . Remarkably, a maximum value of  $t_G$  is about 10 times larger than that obtained for the RPM.

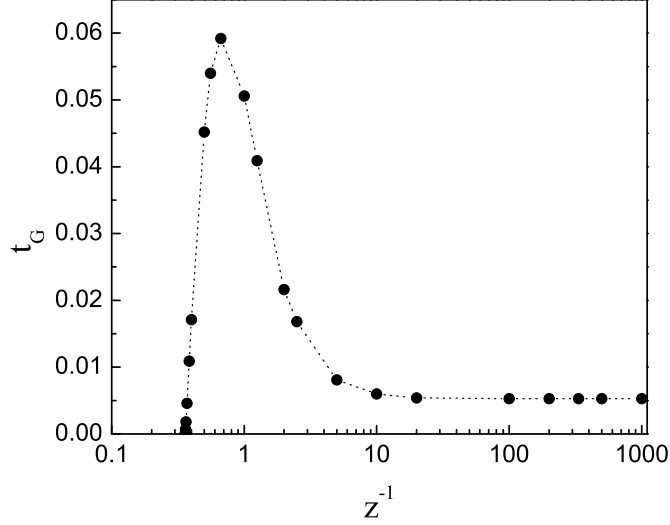


FIG. 9. Reduced Ginzburg temperature as a function of the interaction range  $z^{-1}$ . The line is a guide to the eye.

## V. CONCLUSIONS

Using the approach that exploits the method of CVs we have studied the gas-liquid coexistence and the associated crossover behavior in the screened Coulomb restricted primitive model (YRPM). For this model, we have obtained explicit expressions for all the relevant coefficients of the LG Hamiltonian in a one-loop approximation. Gas-liquid phase diagram, critical parameters and Ginzburg temperature are calculated for  $0.001 \leq z \leq 2.781$  using these expressions. It should be emphasized that the approximation considered produces the mean-field phase diagram.

First, we have studied the dependence of critical temperature and critical density on the interaction range of the Yukawa potential. The critical temperature scaled by the Yukawa potential contact value increases with an increase of the inverse screening length for the whole range of  $z$  for which coexistence exists. The reduced critical density shows a similar trend. Both trends qualitatively agree with the results of simulations [30]. A rapid increase in the critical temperature and density above the corresponding values of the RPM (up to  $z \approx 4$ ) was also found theoretically using the MSA and the GMSA [33, 34].

As for the gas-liquid phase diagram, our results have shown that the region of coexistence in the temperature-density plane reduces with an increase of the inverse screening length  $z$  and completely disappears at  $z > 2.78$ . The trend of the evolution of gas-liquid coexistence

with the variation of  $z$  is generally consistent with the results of computer simulations indicating a stable gas-liquid separation for  $z \leq 4$  [30]. However, the gas-liquid binodal obtained in simulations does not disappear but becomes metastable with respect to the solid-fluid separation for  $z > 4$ . In this study, we have focused exclusively on the gas-liquid equilibrium. The description of transitions involving a solid phase requires going beyond the treatment we have presented here. This issue will be addressed elsewhere.

Finally, we have studied the effect of the interaction region on the crossover behavior by applying the Ginzburg criterion. We have analyzed the coefficients of the LG Hamiltonian as functions of the interaction range. It is significant that for  $z \leq 0.01$ , all the coefficients approach the values obtained for the RPM. It appears that the coefficient  $a_{4,0}$  decreases for  $z > 1.5$  and approaches zero when  $z \simeq 2.78$  indicating the existence of a tricritical point. Accordingly, the reduced Ginzburg temperature tends to zero in this domain of  $z$ . In this case, the tricritical point is the point where the gas-liquid critical point merges with the spinodal branch induced by the charge ordering. The possible existence of a tricritical point for the YRPM with a large  $z$  was discussed in Ref. [4]. For  $z < 2.78$ ,  $t_G$  shows a nonmonotonous behavior. First,  $t_G$  increases reaching a maximum at  $z \simeq 1.5$  and then for  $z < 1.5$ ,  $t_G$  again decreases approaching the RPM value for  $z \simeq 0.01$ . It is interesting to note that the reduced Ginzburg temperature for the YRPM with  $z = 1.8$  is about 10 times larger than  $t_G$  for the RPM ( $z = 0$ ). Therefore, we have found that an increase in the interaction region from the one typical of nonionic fluids to the one typical of ionic fluids leads to a decrease of the temperature region where the crossover from the mean-field critical behavior to Ising model criticality occurs. Extending our previous studies, we have clearly demonstrated that the range of the interactions plays a crucial role in the crossover behavior observed in ionic fluids.

- 
- [1] K. Gutkowski, M.A. Anisimov, and J.V. Sengers, J. Chem. Phys. **114**, 3133 (2001).
  - [2] J.V. Sengers and J.G. Shanks, J. Stat. Phys. **137**, 857 (2009).
  - [3] W. Schröder, Contrib. Plasma Phys. **52** 78 (2012).
  - [4] G. Stell, J. Stat. Phys. **78**, 197 (1995).
  - [5] Y. Levin and M.E. Fisher, Physica A **225**, 164 (1996).



- [6] J.-M. Caillol, Mol. Phys. **103**, 1271 (2005).
- [7] O.V. Patsahan, Condens. Matter Phys **7**, 35 (2004).
- [8] O.V. Patsahan and I.M. Mryglod, J. Phys.: Condens. Matter **16**, L235 (2004).
- [9] A. Ciach, Phys. Rev.E **73**, 066110 (2006).
- [10] A. Parola and D. Pini, Mol. Phys. **109**, 2989 (2011).
- [11] A.-P. Hynninen and A.Z. Panagiotopoulos, Mol. Phys. **106**, 2039 (2008).
- [12] J.-M. Caillol, D. Levesque, and J.-J. Weis, J. Chem. Phys. **116**, 10794 (2002).
- [13] E. Luijten, M.E. Fisher, and A.Z. Panagiotopoulos, Phys. Rev. Lett. **88**, 185701 (2002).
- [14] Y.C. Kim, M.E. Fisher, and A.Z. Panagiotopoulos, Phys. Rev. Lett. **95**, 195703 (2005).
- [15] A. P. Levanyuk, Sov. Phys. JETP **36**, 571 (1959) [Zh. Eksp. Teor. Fiz. **36**, 810 (1959)].
- [16] V.L. Ginzburg, Sov. Phys. Solid State **2**, 1824 (1960) [Fiz. Tverd. Tela **2**, 2031-2043 (1960)].
- [17] P.M. Chaikin and T.C. Lubensky *Principles of condensed matter physics* (Cambridge University Press, 1995).
- [18] M.E. Fisher and Y. Levin, Phys. Rev. Lett. **71**, 3826 (1993).
- [19] M.E. Fisher and B.P. Lee, Phys. Rev. Lett. **77**, 3561 (1996).
- [20] J.F. Leote de Carvalho and R. Evans, J. Phys.: Condens. Matter **7**, L575 (1995).
- [21] W. Schröer and V.C. Weiss, J. Chem. Phys. **109**, 8504 (1998).
- [22] V.C. Weiss and W. Schröer, J. Chem. Phys. **106**, 1930 (1997).
- [23] D.N. Zubarev, Dokl. Acad. Nauk SSSR, **95**, 757 (1954) (in Russian).
- [24] I.R. Yukhnovsky, Sov. Phys. JETP **34**, 263 (1958) [Zh. Eksp. Teor. Fiz. **34**, 379 (1958)].
- [25] I. R. Yukhnovskii and M.F. Holovko, *Statistical Theory of Classical Equilibrium Systems*, (Naukova Dumka, Kiev, 1980) (in Russian).
- [26] O. Patsahan and I. Mryglod, Condens. Matter Phys. **9**, 659 (2006).
- [27] O.V. Patsahan, Phys. Rev. E, **88**, 022102 (2013).
- [28] M.E. Leunissen, C.G. Christova, A.P. Hynninen, C.P. Royall, A.I. Campbell, A. Imhof, M. Dijkstra, R. van Roij, and A. van Blaaderen, Nature, **437**, 235 (2005).
- [29] A.P. Hynninen, M. E. Leunissen, A. van Blaaderen, and M. Dijkstra, Phys. Rev. Lett. **96**, 018303 (2006).
- [30] A. Fortini, A.-P. Hynninen, and M. Dijkstra, J. Chem. Phys. **125**, 094502 (2006).
- [31] M. Bier, R. van Roij, and M. Dijkstra, J. Chem. Phys. **133**, 124501 (2010).
- [32] E.B.El Mendoub, J.-F. Wax, and N. Jakse, J. Chem. Phys. **132**, 164503 (2010).

- [33] R.J.F. Leote de Carvalho and R. Evans, Mol. Phys, **92**, 211 (1997).
- [34] L. Mier-Y-Terán, S.E. Quiñones-Cisneros, I.D. Núñez-Ribini, and E. Lemus-Fuentes, Mol. Phys, **95**,179 (1998).
- [35] J. D. Weeks, D. Chandler, and H.C. Andersen, J. Chem. Phys. **54**, 5237 (1971).
- [36] A. Ciach and G. Stell, J. Mol. Liq., **87**, 255 (2000).
- [37] O.V. Patsahan and I.M. Mryglod, Condens. Matter Phys. **7**, 755 (2004).
- [38] A. Ciach and O. Patsahan, Phys. Rev. E **74**, 021508 (2006).
- [39] B.P. Lee and M.E. Fisher, Phys. Rev. Lett. **76**, 2906 (1996).